Journal of Photochemistry, 8 (1978) 321 - 336

THE KINETICS OF β AND γ BAND QUENCHING IN THE NITRIC OXIDE AFTERGLOW

I. M. CAMPBELL and R. S. MASON
School of Chemistry, The University, Leeds LS2 9JT (Gt. Britain)
(Received November 1, 1977; in revised form November 30, 1977)

Summary

The kinetic behaviours of nitric oxide β and γ band emission intensities associated with combination of $N(^4S) + O(^3P)$ atoms in a discharge–flow system have been examined. Partial replacement of the N_2 carrier with CO_2, O_2, N_2O and H_2O produced quenching behaviour consistent with direct interaction with the emitting states $NO(B^2\Pi)$ ($v' = 0, 1, 2, 3$) and $NO(A^2\Sigma^+)$ ($v' = 0$) as the only effective processes induced. From linear Stern–Volmer-type plots ratios of the quenching rate constant to the radiative rate constant $(k_Q/k_R)/10^4$ dm^3 mol^{-1} were found to be as follows at 298 K:

$NO(B^2\Pi)$

($v' = 0$)			
$(1.1 \pm 0.2)(CO_2)$,	$(16 \pm 3)(O_2)$,	$(24 \pm 5)(N_2O)$,	$(45 \pm 12)(H_2O)$
($v' = 1$)			
$<0.2\ (CO_2)$,	$(3.3 \pm 0.6)(O_2)$,	$(3.8 \pm 0.5)(N_2O)$,	$(8.3 \pm 1.5)(H_2O)$
($v' = 2$)			
$<0.2\ (CO_2)$,	$(2.6 \pm 0.5)(O_2)$,	$(6.1 \pm 0.7)(N_2O)$,	$(8.1 \pm 1.4)(H_2O)$
($v' = 3$)			
$(2.45 \pm 0.22)(CO_2)$,	$(8.5 \pm 2.0)(O_2)$,	$(10.1 \pm 0.9)(N_2O)$,	$(13.3 \pm 2.0)(H_2O)$

$NO(A^2\Sigma^+)$

($v' = 0$)			
$(4.75 \pm 0.24)(CO_2)$,	$(3.2 \pm 0.4)(O_2)$,	$(6.1 \pm 0.7)(N_2O)$,	$(9.8 \pm 1.0)(H_2O)$

Where determinations by other methods were available, the values compared well. In addition unchanged values within the experimental error limits were found for all the above states for O_2 at 195 K. Nitrogen quenched $NO(B^2\Pi)$ ($v' = 3$) with $(k_Q/k_R)/10^4$ dm^3 mol^{-1} equal to 0.28 ± 0.01 at 298 K and 0.40 ± 0.05 at 195 K.

A range of identities of the quenching processes was considered.

1. Introduction

There has been a continuing interest in the study of quenching and energy transfer effects of electronically excited states of small diatomic molecules. In particular, a knowledge of rates of quenching relative to radiation from emitting states has proved vital to the assessment of their population rates and mechanisms in chemiluminescent afterglows. For example in the nitrogen afterglow, under typical conditions, it was shown that the first positive emitting state ($N_2(B^3\Pi_g)$) was predominantly removed by N_2 quenching, and as a consequence that around half the $N(^4S)$ + $N(^4S)$ recombination acts must populate this state [1]. Conversely, in the case of the NO β bands, excited by the $N(^4S)$ + $O(^3P)$ combination, no evidence of quenching by N_2 on $NO(B^2\Pi)$ ($v' = 0$) has been found, so that the radiation rate here is equal to the population rate and results from only a few per cent of associations [2]. This is in keeping with the accepted mechanism involving two precursor species, NO ($a^4\Pi$) and ($b^4\Sigma^-$).

Quenching of the electronically excited doublet states of nitric oxide has been studied using various excitation techniques which thus provides an interesting area for comparison. In the flowing N + O afterglow the $A^2\Sigma^+$, $B^2\Pi$ and $C^2\Pi$ states are populated. However, the A and C states have also been excited in fluorescence and measurements made of the quenching [3, 4], while the B state has been excited by vacuum ultraviolet (VUV) photodissociation of N_2O and subsequent reaction of the product $N(^2D)$ atom [5]. In principle the static methods are simpler than the afterglow method for the study of quenching rates, since a possible problem in the latter is resolution of quenching effects on precursor states from quenching effects on the emitting state itself. Moreover there is a further possibility that increasing mole fractions of quenching gas in the carrier may also lead to different rates of population of emitting states. Accordingly it is one of the aims of this study of the N + O afterglow to resolve these carrier gas effects. At the same time it has proved possible to extend knowledge of the decay parameters for $NO(B^2\Pi)$ through the first four vibrational levels. Of the static methods, the N_2O photodissociation technique has furnished information only for $v' = 0$ while, because of the larger internuclear separation of $NO(B^2\Pi)$ compared with $NO(X^2\Pi)$, fluorescence has been excited only of the $v' = 9$ level [6] which lies above the ground state dissociation limit. Of further interest is a comparison of the quenching parameters of near isoenergetic levels of $NO(A^2\Sigma^+)$ and $(B^2\Pi)$ states; these may reflect the effect of the significantly shorter internuclear separation of the former.

2. Experimental

The essential features of the apparatus and general method have been described in detail before [7, 8] so that only a brief résumé is given here.

Flowing N_2 was partially dissociated by passage through a microwave discharge with flowrates between 100 and 1300 μmol s^{-1} and total pressures

0.1 - 1.4 kPa. The total concentration of $N(^4S)$ atoms was measured by nitric oxide titration at a pepperpot jet just upstream of the observation section, with the familiar reaction represented by

$$N(^4S) + NO \rightarrow N_2 + O(^3P)$$

Partial titration then produced known concentrations of both $N(^4S)$ and $O(^3P)$ in the observation section. In experiments involving mixed carrier gases the other gases (CO_2, N_2O, O_2 and H_2O) were added to the active nitrogen through a side arm upstream of the pepperpot jet.

Chemiluminescent emission intensities were measured along the axis of the observation section from both ends. At the upstream end a collimated beam [8] was detected by an EMI 6256B photomultiplier after passage through optical filters. Nitrogen first positive (1+) intensity ($\propto [N]^2$) was isolated using a Wratten 22 filter. Nitric oxide β band emission intensities were isolated using tuned interference filters (Barr and Stroud Ltd.). At the downstream end radiation was detected by another EMI 6256B photomultiplier mounted on the exit slit of a McPherson Model 218 monochromator purged with dry N_2. The grating had 2400 grooves mm^{-1} and was blazed for about 250 nm. The monochromator was used to isolate individual band emissions of NO in the wavelength range 190 - 500 nm.

The $N(^4S)$ concentration within the observation tube was measured using the calibrated $N_2(1+)$ signals [8] whilst $O(^3P)$ concentrations were calculated from the flowrates of NO added. A titration jet in the exit tubing allowed atom decays along the observation tube to be measured; these were regarded as tolerable if less than 5%. As before [7, 8] experiments could be performed at room temperature or 195 K using Cardice.

During a run the intensity of emissions in the β, γ and δ systems of the NO afterglow were monitored in turn by setting the monochromator to an appropriate wavelength within a selected band. This is equivalent to measuring the integral for the band since profiles are invariant for a defined temperature [7]. Table 1 shows the wavelength settings for the bands in-

TABLE 1
Selected bands and their wavelength settings

Emission system	Band v', v''	Monochromator setting (nm)
δ bands	δ 0,0	191.4
$C^2\Pi \rightarrow X^2\Pi$	δ 0,1	198.0
γ bands	γ 0,1	236.9
$A^2\Sigma^+ \rightarrow X^2\Pi$		
β bands	β 0,5	275.6
$B^2\Pi \rightarrow X^2\Pi$	β 1,13	413.0[a]
	β 2,4	249.0
	β 2,14	421.5[a]
	β 3,3	233.0

[a] Interference filter employed (see text).

vestigated, chosen for high intensity combined with absence of overlap with adjacent bands. Interference filters, centred on wavelengths of 413.0 nm and 421.5 nm and with bandwidths of 2.5 nm and 2.0 nm respectively, proved more suited than the monochromator to the measurement of the weaker intensities which had to be monitored to obtain data on $NO(B^2\Pi)$ $v' = 1$ and $v' = 2$ respectively. Experiments in which the emissions from $v' = 2$ were measured using both the (2,4) band at 249 nm detected by the monochromator and the (2,14) band isolated by the interference filter showed the expected coincident behaviour.

As before [7, 8] the $\delta(0,0)$ band was adopted as an internal standard and the kinetic behaviour of the other bands was obtained from the ratio of their intensity to this standard intensity. This reduces scatter due to any fluctuations of [N] and [O].

For ease of discussion hereafter we shall use the band symbol and a subscript number to denote an electronic state and its vibrational level respectively; thus $\beta_0, \beta_1, \beta_2, \beta_3$ denote $NO(B^2\Pi)$ $v' = 0, 1, 2, 3$ respectively, γ_0 denotes $NO(A^2\Sigma^+)$ $v' = 0$ and δ_0 denotes $NO(C^2\Pi)$ $v' = 0$.

In an earlier paper [7] the atom quenching/enhancement effects on the β bands were reported. The two major effects discovered were significant quenching of β_0 emission with increasing [N] and significant enhancement of β_1 and β_2 with increasing [O]; the last two were shown subsequently to parallel one another [9]. Other smaller effects were usually insignificant under our present conditions but were corrected for where necessary. During the quenching experiments the atom concentrations were usually maintained constant with typical values of $[N] = 2.0 \times 10^{-7}$ mol dm^{-3} and $[O] = 0.6 \times 10^{-7}$ mol dm^{-3}. Within our range of pressures at 298 K the correction factors required to reduce the intensities to zero atom concentrations were 0.7 or greater for β_0 and 1.25 or less for β_1 and β_2, both inversely proportional to the total pressure and dependent upon the carrier gas composition [7].

3. Results

3.1. Nitrogen carriers

The intensity ratios $I(\delta_0)/I(\beta,\gamma)$ are expected to vary with the conditions used here only as a result of variation of the denominator. The δ_0 radiating state, $NO(C^2\Pi)$ $(v' = 0)$, is populated by a preassociation–predissociation equilibrium represented as $N + O \rightleftharpoons NO(C^2\Pi)$ $(v' = 0)$. This state has a short radiative lifetime but the predissociation is much more rapid. The combination of these gives an effective first order rate for depopulation of about 2×10^9 s^{-1} [4]. Accordingly for any quenching molecule under our range of conditions even interaction at the collision frequency could only produce less than 1% decrease in $I(\delta_0)/[N][O]$. Data shown later in Fig. 6 confirm this.

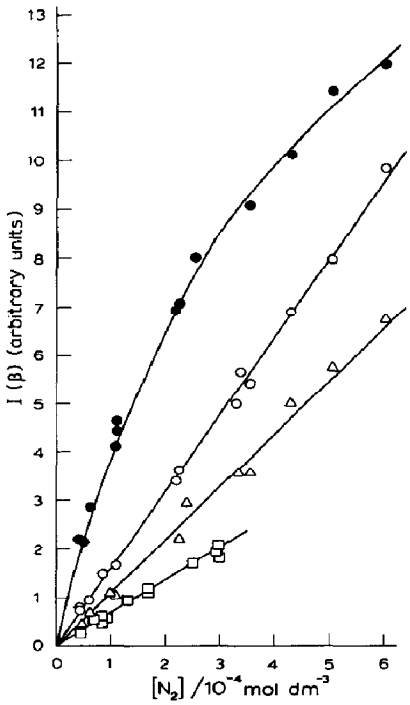

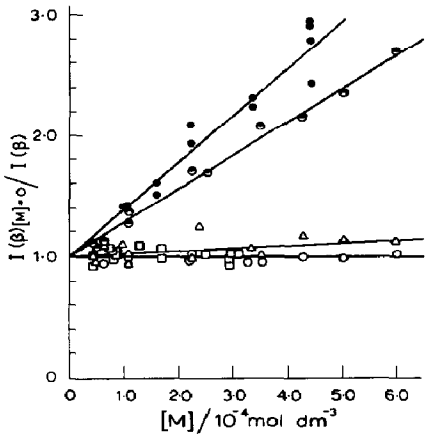

Fig. 1. Plots of the β band intensities *vs.* pressure in N_2 at 298 K: ○, $I(\beta_0)$; □, $I(\beta_1)$; △, $I(\beta_2)$; ●, $I(\beta_3)$.

Fig. 2. Stern–Volmer-type plots of the β band intensities *vs.* total concentration [M] in N_2: ○, β_0, □, β_1, △, β_2, ◒, β_3, all at 298 K; ●, β_3 at 195 K.

Figure 1 shows the variation with total pressure of the intensities of the range of β bands at 298 K, corrected back to zero atom concentrations to eliminate atom quenching and/or enhancement effects. It is clear that β_0, β_1 and β_2 follow a linear pressure relation but that β_3 shows a distinct downward curvature indicative of quenching by N_2. Similar behaviour for β_0 and β_3 has been observed before by Young and Sharpless [10], but they reported a complex pressure dependence for β_1 and β_2 probably because they were unaware of the substantial $O(^3P)$ enhancement effect on these bands.

Figure 2 shows a Stern–Volmer-type of plot for the data of Fig. 1 together with β_3 data for 195 K. The ordinate is the ratio of the measured value of $I(\delta_0)[M]/I(\beta)$ to a value obtained by back extrapolation of the set of such data to zero pressure. This reduced the β_3 data at 298 K from the curve shown in Fig. 1 to a straight line plot (and similarly for the 195 K data).

The variation of $I(\gamma_0)/I(\delta_0)$ with $[N_2]$ at 298 K was a linear plot with a positive intercept, in accord with previous observations [10, 11], indicating a relation

$$\frac{I(\gamma_0)}{[N][O]} = a + b[N_2]$$

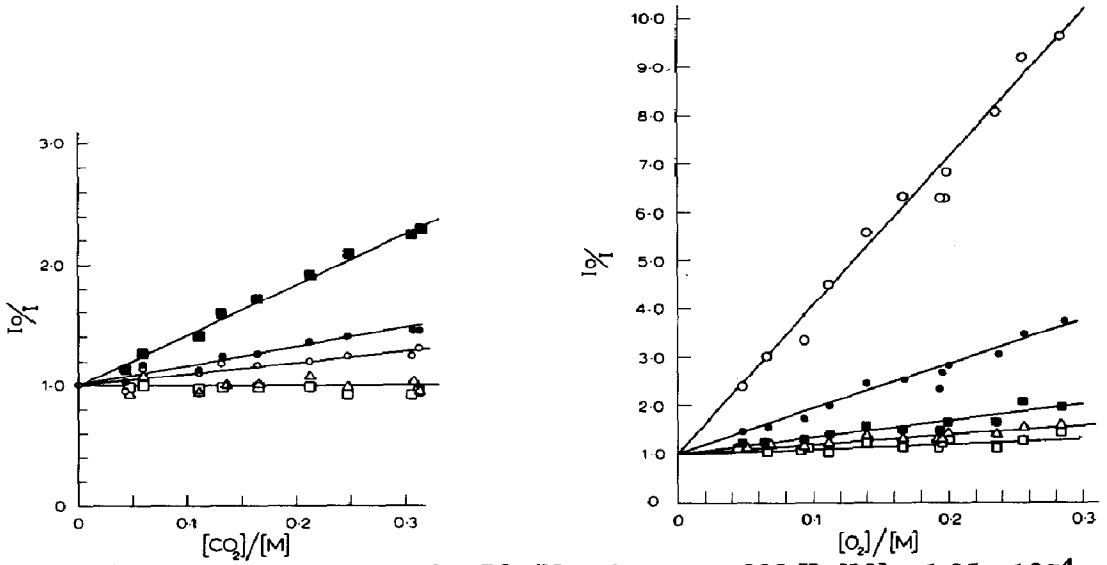

Fig. 3. Stern–Volmer-type plots for CO_2/N_2 mixtures at 298 K, [M] = 1.05×10^{-4} mol dm^{-3}: ○, β_0; □, β_1; △, β_2; ●, β_3; ■, γ_0.

Fig. 4. Stern–Volmer-type plots for O_2/N_2 mixtures at 195 K, [M] = 1.05×10^{-4} mol dm^{-3}: ○, β_0; □, β_1; △, β_2; ●, β_3; ■, γ_0.

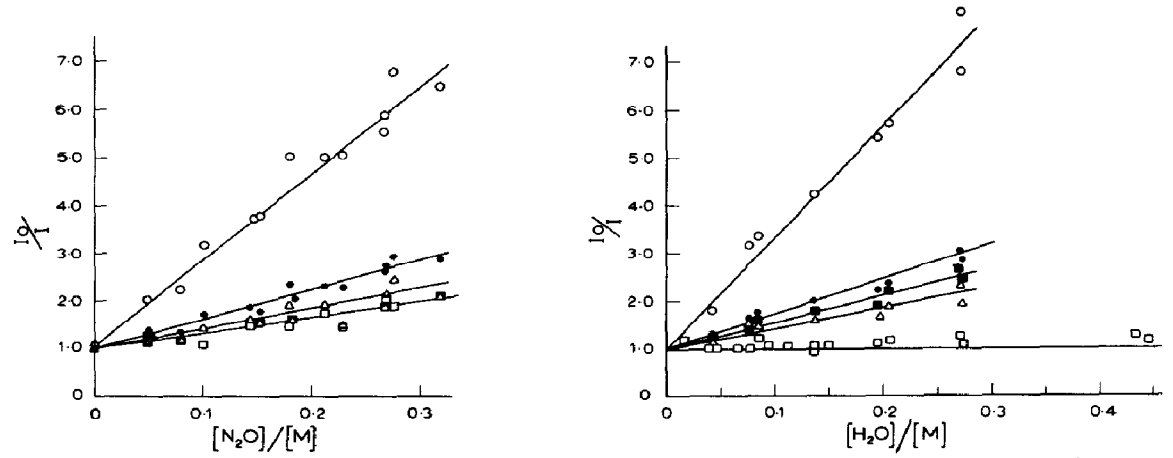

Fig. 5. Stern–Volmer-type plots for N_2O/N_2 mixtures at 298 K, [M] = 0.76×10^{-4} mol dm^{-3}: ○, β_0; □, β_1; △, β_2; ●, β_3. The γ_0 data lie between the β_1 and β_2 data but are omitted here to avoid confusion.

Fig. 6. Stern–Volmer-type plots for H_2O/N_2 mixtures at 298 K, [M] = 0.56×10^{-4} mol dm^{-3}; ○, β_0; △, β_2; ●, β_3. The δ_0 (□) plot contains the data at both [M] = 0.56×10^{-4} and 1.06×10^{-4} mol dm^{-3}. The β_1 data lie beneath the β_2 data and are therefore omitted to avoid confusion.

with a and b constants for a defined temperature. The ratio b/a was found to be $(0.70 \pm 0.06) \times 10^4$ dm^3 mol^{-1} at 298 K, in fairly close agreement with the value of 0.62×10^4 dm^3 mol^{-1} found by Young and Sharpless [10] but lower than the value of 1.15×10^4 dm^3 mol^{-1} found by Gross and Cohen [11]. The absence of any curvature of our plot within the random scatter indicated that quenching of $NO(A^2\Sigma^+)$ ($v' = 0$) by N_2 was insignificant over our range of $[N_2]$.

3.2. Mixed carriers

The effects of the addition of mole fractions of up to about 0.3 of CO_2, O_2, N_2O and H_2O to N_2 carriers on the various band intensities are presented in Stern–Volmer form in Figs. 3, 4, 5 and 6 respectively, with I_0 referring to pure N_2 carrier. All of the plots correspond to quenching and are very close to linear within the small degree of random scatter. It will be shown in the course of the discussion that this is a highly significant observation. In addition the slope to intercept ratios S/I of these plots were measured over a range of total pressures for each gas. Values of S/I[M] proved to be constant within the standard deviation error limits. Even for the most efficient quencher, H_2O, there was clearly no dependence of the S/I[M] ratios over the twofold pressure range investigated (in this case higher pressure experiments were not possible because of difficulty in preserving sufficiently high H_2O flowrates). The only apparent exception was for β_1 emission with O_2 where this ratio decreased by a factor of 5 ± 1.5 at 195 K for [M] increasing from 1×10^{-4} to 4.5×10^{-4} mol dm^{-3} and a factor of 1.8 ± 0.3 at 298 K for [M] increasing from 1×10^{-4} to 2.9×10^{-4} mol dm^{-3}. The β_3 band also showed a much less significant decrease. The H_2O and O_2 data are shown in Table 2. At the higher [M] in H_2O/N_2 mixtures, it was found that some upward curvature of $I(\delta_0)/I(\beta)$ *versus* mole fraction x plots did occur when x was extended to 0.44. Therefore in this case only results for $x \leqslant 0.15$, invariably showing linear behaviour, were analysed.

TABLE 2

Quenching data (S/I[M] $\times 10^4$) as a function of pressure

Quenching gas	Pressure [M] (10^{-4} mol dm^{-3})	Bands				
		γ_0	β_0	β_1	β_2	β_3
H_2O	0.56	9.7 ± 1	42 ± 8	8.4 ± 1.3	8.2 ± 2	13.9 ± 1.4
(298 K)	1.07	9.8 ± 1	49 ± 10	8.2 ± 1	8.0 ± 1.4	12.6 ± 1.3
O_2	1.05	3.0 ± 0.2	19 ± 2	2.6 ± 0.2	2.9 ± 0.3	9.9 ± 0.7
(298 K)	2.92	3.4 ± 0.4	14 ± 5	1.5 ± 0.1	2.4 ± 0.3	7.2 ± 1.2
O_2	1.05	3.0 ± 0.4	27 ± 4	1.0 ± 0.3	1.8 ± 0.2	13.0 ± 1
(195 K)	2.23	3.1 ± 0.2	22 ± 4	0.5 ± 0.1	2.0 ± 0.1	12.0 ± 1.5
	3.36	3.0 ± 0.3	17 ± 8	0.3 ± 0.06	1.5 ± 0.1	10.0 ± 1
	4.44	4.1 ± 0.7	21 ± 3	0.2 ± 0.07	1.8 ± 0.1	8.0 ± 1

4. Discussion

4.1. The population and quenching mechanisms of β band emissions

It is generally accepted that the population mechanism of the emitting states in the nitric oxide afterglow proceeds by initial combination of $N(^4S)$ and $O(^3P)$ atoms into the densely packed vibrational levels of $NO(a^4\Pi)$ close to its dissociation limit. The highest emitting level of $B^2\Pi$ concerned here is $v' = 3$, which lies 47.4 kJ mol^{-1} (0.492 eV) below the first dissociation limit. The only likely mechanism for population of $NO(B^2\Pi)$ involves a combination of vibrational relaxation down the $a^4\Pi$ state and collisional crossing via the $b^4\Sigma^-$ state, the potential curve of which approaches that of $a^4\Pi$ closely on the inner limb and intersects that of $B^2\Pi$ on the outer limb [12]. This means that there are three potential sources of variation of β band emission intensities with addition of substantial mole fractions of the other gases.

(i) Evidently the added gas Q may interact directly with the $B^2\Pi$ state in competition with the radiation rate; this quenching depends on the relative values of the radiative rate constant k_R and $k_Q[Q]$, where k_Q is the quenching rate constant for the species Q.

(ii) The added gas may also quench the precursor state(s) from which population of $NO(B^2\Pi)$ occurs by collisional crossing with rate constant k_c; this quenching depends on the relative values of $k_c[M]$ and $k_q[Q]$, where k_q is the rate constant for quenching of the precursor(s).

(iii) The effective third order rate constant k_1 for population of the precursor states via N + O + M is dependent upon the nature of M, so that rate constants k_{1,N_2} and $k_{1,Q}$ must be distinguished. It may be assumed that this last variation depends upon the mole fraction of Q present.

The above may be summarized in terms of a mechanism based upon the precursor species NO* and emitter NO(B):

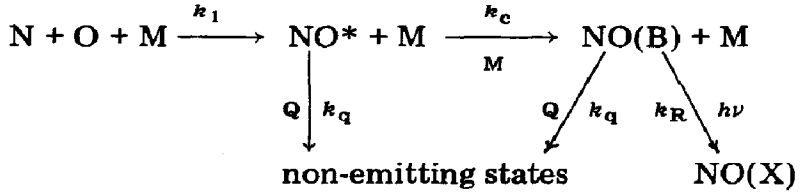

Application of steady state analysis then leads to the prediction for the kinetic behaviour of the reciprocal intensity $I(\beta)$ of the β band:

$$\frac{[N][O]}{I(\beta)} \propto (k_R + k_Q[Q])\left(1 + \frac{k_q}{k_c}\frac{[Q]}{[M]}\right)\frac{1}{k_{1,N_2}[M] + (k_{1,Q} - k_{1,N_2})[Q]}$$

(i) (ii) (iii)

The terms arising from the three mechanistic possibilities above are indicated below the relation. Obviously I_0 (for [Q] = 0) may replace [N][O]

in the above equation preserving the proportionality and indicating the form of the Stern–Volmer-type plot.

Now let us compare the plots of Figs. 3 - 6 with the predicted behaviour. If term (i) is the only one where Q exerts a significant effect, then a linear plot of I_0/I *versus* mole fraction of Q at a fixed total pressure is predicted and the slope to intercept ratio S/I will be equal to $k_Q[M]/k_R$, *i.e.* $S/I[M]$ will be constant for variation of the total pressure and hence of [M]. This is the overwhelming behaviour observed.

4.2. Comparison of results with predicted behaviour

We have shown that the Ogawa band intensities from $NO(b^4\Sigma^-)$ levels are consistent only with a mechanism where pressure dependent processes rather than radiative decay are overwhelmingly responsible for depopulation of this precursor species under similar conditions to those used here [8]. Thus if term (ii) is significant alone we can be sure that the gradient of a plot of I_0/I *versus* [Q]/[M] will be k_q/k_c, a constant, and $S/I[M]$ will simply be inversely proportional to [M], which disagrees with the results of Table 2, apart from β_1 quenching by O_2. There is a decrease in the β_3 O_2 (195 K) data, which, however, corresponds only to about 40 ± 10% change over a pressure change of 450%. There is clearly no direct inverse proportionality, although in this case the change could reflect a small contribution from quenching by O_2 of the direct precursor to β_3.

If process (ii) were operative in conjunction with process (i), this would lead to a quadratic term in [Q] in the Stern–Volmer plot prediction and hence Figs. 3 - 6 would show strong upward curvature. Only in the case of large mole fractions of H_2O (about 0.44) was any such curvature in evidence, when we conclude that some minor quenching was occurring on the precursor species. This is in keeping with our observation [8] that H_2O is considerably more efficient than either N_2O or CO_2 in quenching $NO(b^4\Sigma^-)$, the likely precursor concerned.

It is unlikely that term (iii) operates in isolation since CO_2, N_2O and H_2O would be expected to be more efficient third bodies than N_2 if anything. However, if term (iii) operates in conjunction with (i), it should lead to downward curvature of the Stern–Volmer plots, which is not observed. Thus the strong linearity of our plots in Figs. 3 - 6 provides good evidence that the effective rate constant for three-body combination into the precursor state(s) is independent of carrier-gas composition within the mole fraction ranges considered here. This represents a contrast with the overall rate constant for the three-body association of N + O where at room temperatures the relative efficiencies of CO_2 and N_2O are 3.01 and 2.25 respectively compared with 1.0 for N_2 [13]. In their study of CO_2 and N_2O quenching of β_0 emission Campbell and Thrush [2] assumed that such efficiencies also applied to the rate constant for population of the precursor(s), which is now disproved.

Apart from the apparently odd kinetic behaviour of β_1 with O_2 addition, we find all our evidence on β emission consistent with the added gases

TABLE 3

$k_Q/k_R \times 10^{-4}$ dm^3 mol^{-1}

Quenching gas	Temperature (K)	γ_0	β_0	β_1	β_2	β_3
N_2	298	0.0014 [4] <0.002 [28] 0.006 [29]	0.11 [5]		0.03±0.01	0.3±0.01
	195				0.04±0.02	0.4±0.05
CO_2	298	4.8±0.3 4.7±0.5 [4] 4.2 [10] 2 [31] 0.7 [32] 4 [33] 6 [3]	1.1±0.2 1.3 [5] 1.9 [2]			2.5±0.3
O_2	298	3.2±0.4 1.9±0.2 [14]	16.3±3 29.7±6 [5]	(3.3±0.6)	2.7±0.5	8.5±2
	195	3.2±0.4	21±3	(1.5±0.3)	1.8±0.4	11.5±3
N_2O	298	6.1±0.7 6.5 [10,15]	24±5 6±2 [5] 8.4 [2]	3.8±0.5	6.1±0.7	10±1
H_2O	298	10±1 6 [27] 4 [28]	45±12	8±2	8±2	13±2

directly quenching the emitting state as the origin of the overwhelming effect for mole fractions of 0.3 or less. On this basis we can evaluate k_Q/k_R values directly from the slope to intercept ratios of Figs. 3 - 6. Similar arguments apply to the γ_0 emission intensities where the linearity of the Stern–Volmer plots can only be consistent with quenching upon the $A^2\Sigma^+$ state and again we may deduce k_Q/k_R simply from the slope to intercept ratio of the plots. Thus we have set out our values of k_Q/k_R in Table 3 together with the values obtained by the static techniques for comparison. Included in Table 3 are our O_2 quenching data for the β_1 band obtained on the assumption that the true value of k_Q/k_R is that produced by back-extrapolation of the downward sloping S/I[M] *versus* [M] plots to [M] = 0. Because we cannot justify this procedure in terms of a defined mechanism, these numbers appear in parentheses. The error introduced by the small pressure effect on β_3 is within the standard deviation quoted.

In Table 3 it can be seen that there is excellent agreement of our value of k_Q/k_R for CO_2 and the γ_0 state with that obtained by Callear and Pilling [4] by the fluorescence method, with ours better defined. The values obtained by Young and Sharpless [10] in a flowing afterglow are also close but are just beyond our error limits, while their values of k_Q/k_R for N_2O

TABLE 4

k_Q (10^9 dm^3 mol^{-1} s^{-1})

Quencher	Temperature (K)	$A^2\Sigma^+$	$B^2\Pi$			
		$v' = 0$	$v' = 0$	1	2	3
		$k_R/10^5$ s^{-1} [17]				
		22.2	3.23	4.35	4.55	4.55
N_2	298		—	—	0.1±0.06	1.27±0.05
	195		—	—	0.18±0.09	1.8 ±0.25
CO_2	298	105±5	3.6±0.7	—	—	11±1
O_2	298	70±9	53±10	(14)	12±2	39±9
	195	70±9	68±10	(7)	8±2	52±14
N_2O	298	135±15	76±16	16±2	28±4	46±5
H_2O	298	218±22	145±39	36±7	37±6	61±9

and γ_0 are in good agreement with ours. In the case of O_2 and γ_0 our value of k_Q/k_R is somewhat higher than that obtained by Melton and Klemperer [14] in a fluorescence method. The invariance of our values for 298 K and 195 K is not unexpected since combination with the radiative rate constant for the γ_0 state (Table 4) suggests that O_2 quenches NO($A^2\Sigma^+$) ($v' = 0$) at around half the collision frequency.

Quenching parameters for NO($B^2\Pi$) ($v' = 1, 2, 3$) with different gases have not been obtained before. For $v' = 0$ the main comparison is with the values obtained by Black *et al.* [5] using VUV photodissociation of N_2O as source. One immediate problem is that they found an apparent k_Q/k_R for N_2 itself which should have produced strong curvature of our β_0 plot of Fig. 1 if it were real (*cf.* the β_3 plot). The other comparisons for β_0 are not in wide disagreement: for CO_2 the values of k_Q/k_R are almost the same, for O_2 our value is lower by almost a factor of 2 while for N_2O our value is about four times higher. There is no obvious source of error in either technique, but it may be said that the production of NO($B^2\Pi$) ($v' = 0$) in the system of ref. 5 involves a secondary reaction of a highly reactive intermediate species N(^{2}D) and also that the filter used (300 - 400 nm transmission) was not particularly selective for β_0 emission.

4.3. Absolute values of quenching rate constants

In order to convert the data of Table 3 into absolute values of k_Q absolute values of k_R for each level are required. Radiative lifetimes of the vibrational levels of the NO($A^2\Sigma^+$) state have been measured by a number of workers [16 - 22] and values obtained for the same vibrational level have differed by a factor of up to 4. This indicates the uncertainties that can attach to k_R values. Only one determination of the radiative lifetimes of

$NO(B^2\Pi)$ levels is available [17]. Table 4 then represents the array of absolute values of k_Q rate constants derived from our work. Since we are interested in comparing relative values of k_Q for both the $A^2\Sigma^+$ and $B^2\Pi$ states we have used the only complete set of k_R values determined for all the levels concerned here [17] in preference to perhaps better but isolated estimates. However, it follows that the absolute values in the table may only be accurate to within a factor of 2.

4.4. The nature of the quenching processes

There are four general quenching mechanisms which could be operative:

(a) direct energy transfer from NO(A,B) to the quenching molecule which may or may not dissociate as a result;

(b) near isoenergetic transfer from the NO(A,B) potential curve to another electronic state of NO with little energy transferred to the quenching molecule;

(c) chemical reaction of the excited NO species with the quenching gas as exemplified by the process detected by Cohen and Heicklen [23] from photolysis work

$$NO(A^2\Sigma^+) + CO_2 \rightarrow NO_2 + CO$$

(d) an energy exchange process involving a substantial degree of electronic to electronic energy transfer so exciting the quenching molecule to an electronically excited state.

We may commence our discussion with the N_2 quenching observed only for $NO(B^2\Pi)$ ($v' = 3$) with certainty. The most striking differentiation of the behaviour of this vibrational level from that of the lower ones might suggest the crossing of a threshold for electronic excitation of N_2; however, the energy required to excite $N_2(A^3\Sigma_u^+)$ ($v' = 0$) is 597.2 kJ mol^{-1} while the excitation energy of $NO(B^2\Pi)$ ($v' = 3$) is only 579.8 kJ mol^{-1} and the deficit is too large to be made up by thermal energy. However, a second mechanism is suggested by our recent paper [8] which located the energy of $NO(b^4\Sigma^-)$ ($v' = 1$) (Gilmore's numbering scheme [12]) as being between 575 and 580 kJ mol^{-1}. This level then lies very close to $NO(B^2\Pi)$ ($v' = 3$) so that the process induced by N_2 may be of type (b). The wider vibrational spacing in NO(b) (120 000 m^{-1}) compared with NO(B) (99 600 m^{-1}) means that the $v' = 0$ level of the former state lies almost between $v' = 1$ and $v' = 2$ of NO(B) so that N_2 can no longer induce effective curve crossing. Thus a type (b) mechanism seems the most likely explanation here and may well extend to part of the quenching on NO(B) ($v' = 3$) induced by CO_2 where k_Q is around three times larger than for $v' = 0$. However, it is also necessary to consider mechanisms of types (a) and (c) for CO_2, since D(O—CO) $\approx$ 532 kJ mol^{-1} and the excitation energy of NO(B) ($v' = 0$) is 544.2 kJ mol^{-1}. Both mechanisms are probably also open to NO(A) ($v' = 0$) even though the excitation energy is only 528.6 kJ mol^{-1}, since thermal energy could make up the difference for a type (a) mechanism. Mechanism (c) has in fact been demon-

strated to occur [23] with the A state, and yet the ratios of k_Q values for NO(A) ($v' = 0$) to those for NO(B) ($v' = 0, 3$) are the greatest seen in Table 4.

For the other quenching gases, O_2, N_2O and H_2O, the primary bond energies are all low enough to permit dissociation by energy transfer from all of the states concerned here. Of possible significance for these is that the k_Q values for NO(B) ($v' = 3$) are now lower than those for NO(B) ($v' = 0$), while the latter values are at most only a factor of 2 lower than the corresponding k_Q values for NO(A) ($v' = 0$), in contrast to the relative magnitudes for CO_2 and to some extent N_2.

4.5. Conservation of internuclear separation

This all suggests that factors other than mere energy requirements are important, in particular the accessibility of the electronic energies for quenching interactions. For instance, in order for the full excitation energy of NO(B) ($v' = 0$) to be applied, taking the NO down to $X^2\Pi$ ($v' = 0$), it is necessary that the bond separation of NO be compressed by a relatively large amount (0.04 nm). In contrast, the bottoms of the A and X potential curves lie at similar internuclear separations, so that it could be argued that the full excitation energy of NO(A) ($v' = 0$) is more accessible than those of NO(B) levels. In optical transitions the relative accessibility of excitation energy for conversion to radiative energy is governed in the main by Franck–Condon factors. Now although energy transfer induced by collision involves perturbations not concerned in optical transitions, there is considerable evidence for the conservation of internuclear separations in electronic energy transfer processes and at least a partial validity of Franck–Condon factors in determining rates. Instances are energy transfer from $N_2(A^3\Sigma_u^+)$ [24 - 26], high energy ion–molecule collisions [27, 28] and Penning ionization collisions [29].

If it is presumed that the quenching processes observed here actually involve an energy transfer represented by

$$NO(A,B)v' + Q \rightarrow NO(X)v'' + Q(*)$$

in which the energy transferred is $\Delta E' = E_{v'} - E_{v''}$, then for all the processes involving $\Delta E' \geqslant 350$ kJ mol^{-1} the sum of the Franck–Condon factors from Nicholls' tables [30] is significantly lower (a factor of 2 or more) for NO(B) ($v' = 0 - 3$) than for NO(A) ($v' = 0 - 3$). This comparison appears to be best developed in the case where Q is CO_2 where, if we regard the sole process as that producing dissociation of CO_2, a $\Delta E'$ greater than 529 kJ mol^{-1} is required in addition to thermal energy. Table 5 shows the sum of Franck–Condon factors for all transitions of each level equivalent to this energy or more, bringing in the NO($C^2\Pi$) ($v' = 0$) state also, in comparison with the corresponding k_Q values. It can be seen that the general order of k_Q follows the Franck–Condon factor sums but that the correspondence is no stronger than that. Extending the argument to the other molecules, regarding the O—O, N_2—O and H—OH bond energies as defining $\Delta E'$ approximately in the

TABLE 5

Comparison of Franck–Condon factor sums with k_{CO_2} values

Excited state	$\Sigma F/C_{v' \rightarrow v''}$, where $E_{v'} - E_{v''} \geq 528$ kJ mol^{-1}	k_{CO_2} (10^{10} dm^3 mol^{-1})
NO $C^2\Pi$ $v' = 0$	0.9	200[a]
$A^2\Sigma^+$ $v' = 3$	0.44	19[a]
$v' = 0$	0.17	24[b]
$B^2\Pi$ $v' = 3$	0.07	1.1[b]
$v' = 2$	0.008	—
$v' = 1$	0.002	—
$v' = 0$	2×10^{-5}	0.4[b]

[a]Ref. 4. [b]This work.

respective cases, the sum of the Franck–Condon factors for NO(A) ($v' = 0$) always exceeds those for each of the NO(B) levels, again in agreement with the k_Q data. Also predicted on this basis is the substantial increase of the ratio of k_Q for NO(B) $v' = 0$ over $v' = 3$ compared with CO_2, while k_Q for NO(A) ($v' = 0$) does not change dramatically.

The Franck–Condon factor argument revolves around only type (a) quenching mechanisms, and we have mentioned earlier evidence for type (b) and (c) mechanisms which must detract from the strength of the argument. Moreover for O_2 at least there is a possibility of a type (d) quenching mechanism for NO(B) which does not appear to be open for NO(A). The bottom of the NO($a^4\Pi$) potential curve lies almost directly below that of NO($B^2\Pi$) [12] (shown as Fig. 6 in ref. 8) and so is at a much larger internuclear distance than NO($A^2\Sigma^+$). On this basis there is an almost exact energy resonance for a process represented by

$$NO(B^2\Pi)\ (v' = 0) + O_2(X^3\Sigma_g^-)\ (v'' = 0) \rightarrow NO(a^4\Pi)\ (v'' = 0) + O_2(a^1\Delta_g)\ (v' = 0)$$

The excitation energy of $O_2(a^1\Delta_g)$ is 93 kJ mol^{-1}, while the energy difference of the NO vibronic states is 91 kJ mol^{-1}. Moreoever, the process is spin allowed and Franck–Condon factors in both molecules should be highly favourable. N_2O and H_2O quenching of NO($B^2\Pi$) ($v' = 0$) could also be based on deactivation to NO($a^4\Pi$) and this could also be an origin of the large k_Q values. However, this will be less important as v' increases since the NO($a^4\Pi$) potential curve is very shallow in comparison with NO($B^2\Pi$) so that the Franck–Condon factor sums will fall off rapidly. Thus this mechanism could be at least part of the explanation for the decreased values of k_Q for $v' = 1$, 2 compared with $v' = 0$ in NO($B^2\Pi$) and the approach of k_Q for $v' = 0$ for NO($B^2\Pi$) to k_Q for NO(A^{2+}) ($v' = 0$) evident in Table 4.

5. Conclusions

The quenching of β and γ bands by N_2, CO_2, O_2, N_2O and H_2O has been investigated. The behaviour observed is consistent with direct interaction of the quencher with the emitting state itself, any effects of quenching on the precursor states being small.

The more direct fluorescence methods of quenching studies have not proved to be feasible for studying the NO β bands. However, comparison of the present quenching rate data with those measured by other techniques suggest that the present method is better in the sense that we have extended quenching measurements to vibrational levels of $NO(B^2\Pi)$ above $v = 0$.

A range of identities of the quenching processes have been considered and it has been found that the sum of the Franck–Condon factors for NO transitions of sufficient energy to dissociate or induce electronic transitions in the quenching molecules can predict the general order of reactivities. Nitrogen quenching of $NO(B^2\Pi)$ ($v' = 3$) can only be explained as collision-induced crossing into a nearby isoenergetic $NO(b^4\Sigma^-)$ vibrational level.

Acknowledgment

The authors acknowledge a considerable contribution to the interpretations advanced in this paper by the preliminary studies of Dr. S. B. Neal.

References

1 I. M. Campbell and B. A. Thrush, Proc. R. Soc. London, Ser. A, 296 (1967) 202.
2 I. M. Campbell and B. A. Thrush, J. Quant. Spectrosc. Radiat. Trans., 8 (1968) 1571.
3 A. B. Callear and I. W. M. Smith, Trans. Faraday Soc., 59 (1963) 1720.
4 A. B. Callear and M. J. Pilling, Trans. Faraday Soc., 66 (1970) 1618.
5 G. Black, R. L. Sharpless and T. G. Slanger, J. Photochem., 5 (1976) 435.
6 T. Hikida, S. Nakajima, T. Ichimura and Y. Mori, J. Chem. Phys., 65 (1976) 1317.
7 I. M. Campbell and S. B. Neal, Discuss. Faraday Soc., 53 (1972) 72.
8 I. M. Campbell and R. S. Mason, J. Photochem., 5 (1976) 383.
9 I. M. Campbell and R. S. Mason, to be published.
10 R. A. Young and R. L. Sharpless, Discuss. Faraday Soc., 33 (1962) 228.
11 R. W. F. Gross and N. Cohen, J. Chem. Phys., 48 (1968) 2582.
12 F. R. Gilmore, J. Quant. Spectrosc. Radiat. Trans., 5 (1965) 369.
13 I. M. Campbell and B. A. Thrush, Proc. R. Soc. London, Ser. A, 296 (1967) 222.
14 L. A. Melton and W. Klemperer, Planet. Space Sci., 20 (1972) 157.
15 J. Heicklen and N. Cohen, Adv. Photochem., 5 (1968) 157.
16 B. M. Weinstock and R. N. Zare, J. Chem. Phys., 56 (1972) 3456.
17 M. Jeunehomme and A. B. F. Duncan, J. Chem. Phys., 41 (1964) 1692.
18 M. Jeunehomme, J. Chem. Phys., 45 (1966) 4433.
19 G. E. Copeland, J. Chem. Phys., 56 (1972) 689.
20 H. Bubert and F. W. Froben, Chem. Phys. Lett., 8 (1971) 242.
21 J. Brzozowski, N. Elander and P. Erman, Phys. Scr., 9 (1974) 99.
22 H. Zacharias, J. B. Halpern and K. H. Welge, Chem. Phys. Lett., 43 (1976) 41.
23 N. Cohen and J. Heicklen, J. Phys. Chem., 71 (1967) 558.

24 D. H. Stedman and D. W. Setser, J. Chem. Phys., 52 (1970) 3957.
25 A. B. Callear and P. W. Wood, Trans. Faraday Soc., 67 (1971) 272.
26 E. M. Gartner and B. A. Thrush, Proc. R. Soc. London, Ser. A, 346 (1975) 121.
27 J. H. Moore and J. P. Doering, Phys. Rev., 177 (1969) 218.
28 R. S. Lehrle and R. S. Mason, Int. J. Mass Spectrom. Ion Phys., 21 (1976) 165.
29 W. W. Robertson, J. Chem. Phys., 44 (1966) 2456.
30 R. W. Nicholls, J. Res. Nat. Bur. Stand., Sect. A, 68 (1964) 535.
31 A. V. Kleinberg and A. N. Terenin, Dokl. Akad. Nauk SSSR, 101 (1955) 1031.
32 N. Basco, A. B. Callear and R. G. W. Norrish, Proc. R. Soc. London, Ser. A, 260 (1961) 459.
33 H. P. Broida and T. Carrington, J. Chem. Phys., 38 (1963) 136.